AN ALTERNATIVE DERIVATION OF CLASSIC CONING MOTION VIA EULER ANGLES

Jacques Waldmann
Instituto Tecnológico de Aeronáutica - Department of Systems and Control - 12228-900 - São José dos Campos - SP - Brazil
e-mail: jacques@ele.ita.br

Abstract. *A novel alternative derivation of classic coning motion based on Euler angles is presented. This particular motion is often used to assess candidate attitude determination algorithms for strapdown inertial navigation systems. The derivation is based on rotating the body coordinate frame according to time-varying Euler angles related with body precession, spin rate, and cone half-angle while the rotation vector remains orthogonal to the plane containing both the spin axis and the precession axis. Consequently, for a desired cone half-angle and precession rate, the required spin rate vector is dictated by the precession vector. The derivation builds on geometry-based reasoning that provides an insight into how classic coning motion develops in space.*

Keywords*. Coning motion, rotation vector, Euler angles, attitude determination, inertial navigation.*

1. Introduction

Strapdown inertial navigation systems produce estimates of terrestrial position and velocity from specific force and angular rate data provided by an inertial measurement unit rigidly attached to the vehicle body. It requires the computation of the rotation matrix $\mathbf{C}_\mathbf{n}^\mathbf{b}$ that transforms specific force sensed by the accelerometers from body frame S_b to navigation frame S_n. The computation uses body-fixed rate gyro measurements to determine the body angular rate with respect to the navigation frame. The computation of $\mathbf{C}_\mathbf{n}^\mathbf{b}$, known as the attitude determination problem, calls for the solution of (Bortz, 1971):

$$\dot{\mathbf{C}}_\mathbf{n}^\mathbf{b} = \mathbf{C}_\mathbf{n}^\mathbf{b}\begin{bmatrix} 0 & -\omega_{zb} & \omega_{yb} \\ \omega_{zb} & 0 & -\omega_{xb} \\ -\omega_{yb} & \omega_{xb} & 0 \end{bmatrix} = \mathbf{C}_\mathbf{n}^\mathbf{b}\{\boldsymbol{\omega}_\mathbf{nb}^\mathrm{b}\}\;;\quad \mathbf{C}_\mathbf{n}^\mathbf{b}(0) = \mathbf{C_0} \tag{1}$$

where $\boldsymbol{\omega}_\mathbf{b}^\mathbf{bn} = \begin{bmatrix}\omega_{xb} & \omega_{yb} & \omega_{zb}\end{bmatrix}^T$ is the angular rate vector of the body frame relative to the navigation frame represented in the body frame. Attitude determination algorithms numerically solve Eq. (1), often using angular rate data in the form of incremental angles. A major problem lies in the noncommutativity of finite rotations The differential equation and corresponding rotation matrix, respectively, of the rotation vector $\mathbf{r}$ that aligns the reference frame S_n with body frame S_b are clearly shown in Eqs. (2-3) (Bortz, 1971; Ignagni, 1990, 1994; Jiang, 1991, 1992; Lee, 1990; Lovren, 1998; Miller, 1983; Shuster, 1993):

$$\dot{\mathbf{r}} = \boldsymbol{\omega}^\mathbf{bn} + \frac{1}{2}\mathbf{r}\times\boldsymbol{\omega}^\mathbf{bn} + \frac{1}{r^2}\left[1-\frac{r\sin(r)}{2(1-\cos(r))}\right][\mathbf{r}\times(\mathbf{r}\times\boldsymbol{\omega}^\mathbf{bn})] \qquad r = |\mathbf{r}| \qquad \mathbf{r}_{kT} = \mathbf{0} \tag{2}$$

$$\mathbf{C}_\mathbf{n}^\mathbf{b}((k+1)T) = \mathbf{C}_\mathbf{n}^\mathbf{b}(kT)\left[\mathbf{I} + \frac{\sin(r_{(k+1)T})}{r_{(k+1)T}}\{\mathbf{r}_{(k+1)T}\} + \frac{1-\cos(r_{(k+1)T})}{r_{(k+1)T}^2}\{\mathbf{r}_{(k+1)T}\}^2\right] \tag{3}$$

The noncommutativity rate vector consists of the last two terms in the right-hand side of Eq. (2). Previous work numerically solved approximations to the rotation vector differential equation at a fast rate in the interval $t\in[kT,(k+1)T)$ from null initial conditions at the beginning of every interval T, and updated the rotation matrix in Eq. (3), or its corresponding rotation quaternion, at a slower rate to reduce the computational workload (Ignagni, 1990, 1994; Jiang, 1992; Lee, 1990; Miller, 1983).

From Eq. (2), one notices that the attitude determination algorithm is tested under worst conditions when, given $|\boldsymbol{\omega}|$ and $|\mathbf{r}|$, these vectors are orthogonal. This reference motion is known as classic coning (Bortz, 1971; Jiang, 1991). It has been used as an example of the application of Eq. (2) (Jiang, 1991), and in the optimization and evaluation of attitude determination algorithms (Bortz, 1971; Ignagni, 1990, 1994; Jiang, 1992; Lee, 1990; Lovren, 1998; Miller, 1983). A particular rotation vector history was substituted in Eq. (2), yielding the angular rate of the desired classic coning motion (Bortz, 1971; Jiang, 1991). A quaternion-based derivation can be found in (Miller, 1983). However, previous work on attitude determination lacks a clear, physically intuitive description of the temporal evolution in three-dimensional (3D) space of a body undergoing classic coning motion.

The focus here is on the derivation of classic coning motion to provide an insight into the body evolution in 3D space. The derivation builds on the direction cosine matrix that results from rotating the body coordinate frame according to appropriate Euler angles. The Euler angles are related to precession rate vector $\Omega\hat{\mathbf{z}}_{\mathbf{n}}$, cone half-angle r, and body spin rate vector $\dot{\phi}\hat{\mathbf{z}}_{\mathbf{b}}$. Figure 1 depicts the fixed reference frame $S_n=\{\hat{\mathbf{x}}_{\mathbf{n}},\hat{\mathbf{y}}_{\mathbf{n}},\hat{\mathbf{z}}_{\mathbf{n}}\}$. The body frame $S_b=\{\hat{\mathbf{x}}_{\mathbf{b}},\hat{\mathbf{y}}_{\mathbf{b}},\hat{\mathbf{z}}_{\mathbf{b}}\}$ is depicted only by $\hat{\mathbf{z}}_b$ for the sake of simplicity. The body rotates about its spin axis $\hat{\mathbf{z}}_b$, which simultaneously precesses about axis $\hat{\mathbf{z}}_n$ and maintains a constant cone half-angle angle r. It will be seen that classic coning motion constrains the rotation vector **r** to be orthogonal to both the precession axis $\hat{\mathbf{z}}_n$ and the body spin axis $\hat{\mathbf{z}}_b$. The orthogonality constraint imposes that a condition be satisfied by the spin rate vector $\dot{\phi}\hat{\mathbf{z}}_{\mathbf{b}}$. Evaluation of candidate attitude determination algorithms under the conditions of classic coning motion is then straightforward: the representation of the angular rate in body frame coordinates, namely $\boldsymbol{\omega}_b^{bn}$, is employed as the ground-truth input signal to the strapdown rate gyros when simulating the operation of a strapdown navigation system ((Bortz, 1971; Ignagni, 1990, 1994; Jiang, 1992; Lee, 1990; Lovren, 1998; Miller, 1983).

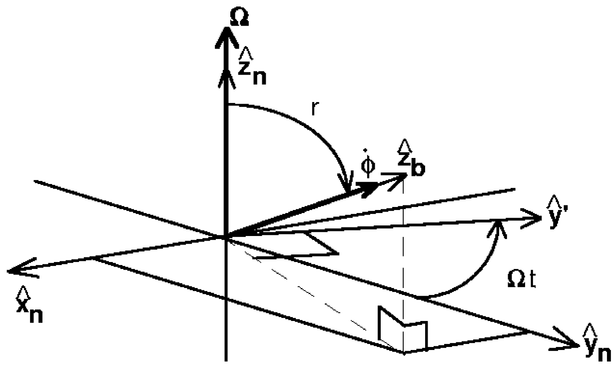

Figure 1 - Coning motion: body spins with rate $\dot{\phi}$ about its spin axis $\hat{\mathbf{z}}_{\mathbf{b}}$, which simultaneously precesses with rate Ω about precession axis $\hat{\mathbf{z}}_{\mathbf{n}}$.

2. Derivation of Coning Motion

The following sequence of Euler angles rotate the reference frame S_n into alignment with body frame S_b :

$$S_n \rightarrow \Omega t\hat{\mathbf{z}}_n \rightarrow r\hat{\mathbf{y}}' \rightarrow \dot{\phi}t\hat{\mathbf{z}}_b \rightarrow S_b \tag{4}$$

where the hat superscript indicates unit magnitude. The cone half-angle r between $\hat{\mathbf{z}}_b(t)$ and $\hat{\mathbf{z}}_n$ is represented as a rotation about the intermediate unit vector $\hat{\mathbf{y}}'(t)$, as shown in Figure 1. From the corresponding piogram (Pio, 1966), the direction cosine matrix that transforms from S_n to S_b is:

$$\mathbf{C}_b^n = \begin{bmatrix} c(\Omega t)c(r)c(\dot{\phi}t) - s(\Omega t)s(\dot{\phi}t) & s(\Omega t)c(r)c(\dot{\phi}t) + c(\Omega t)s(\dot{\phi}t) & -s(r)c(\dot{\phi}t) \\ -c(\Omega t)c(r)s(\dot{\phi}t) - s(\Omega t)c(\dot{\phi}t) & -s(\Omega t)c(r)s(\dot{\phi}t) + c(\Omega t)c(\dot{\phi}t) & s(r)s(\dot{\phi}t) \\ c(\Omega t)s(r) & s(\Omega t)s(r) & c(r) \end{bmatrix} \tag{5}$$

The precession rate vector is represented in S_b as:

$$\boldsymbol{\omega}_b = \mathbf{C}_b^n\boldsymbol{\omega}_n = \mathbf{C}_b^n\begin{bmatrix} 0 \\ 0 \\ \Omega \end{bmatrix} = \begin{bmatrix} -\Omega s(r)c(\dot{\phi}t) \\ \Omega s(r)s(\dot{\phi}t) \\ \Omega c(r) \end{bmatrix} \tag{6}$$

and hence the body angular rate vector representation in S_b becomes:

$$\boldsymbol{\omega}_b^{bn} = \boldsymbol{\omega}_b + \begin{bmatrix} 0 \\ 0 \\ \dot{\phi} \end{bmatrix} = \begin{bmatrix} -\Omega s(r)c(\dot{\phi}t) \\ \Omega s(r)s(\dot{\phi}t) \\ \Omega c(r) + \dot{\phi} \end{bmatrix} \tag{7}$$

By definition, classic coning motion must yield a rotation vector $\mathbf{r}$(t) orthogonal to $\boldsymbol{\omega}^{\mathbf{bn}}$ – therefore to both components of $\boldsymbol{\omega}^{\mathbf{bn}}$ in the right-hand side of the first equality in Eq. (7). Hence, $\mathbf{r}$(t) must be orthogonal to both the spin and precession axes, $\hat{\mathbf{z}}_{\mathrm{b}}$(t) and $\hat{\mathbf{z}}_{\mathrm{n}}$, respectively. In other words, $\mathbf{r}$(t) is orthogonal to the rotating plane $\hat{\mathbf{z}}_{\mathbf{b}}\hat{\mathbf{z}}_{\mathbf{n}}$ precessing with rate $\Omega\,\hat{\mathbf{z}}_{\mathrm{n}}$. Consequently, $\mathbf{r}$(t) is in the intersection of plane $\hat{\mathbf{x}}_{\mathbf{n}}\hat{\mathbf{y}}_{\mathbf{n}}$ with the rotating plane $\hat{\mathbf{x}}_{\mathbf{b}}\hat{\mathbf{y}}_{\mathbf{b}}$, the latter also precessing with rate $\Omega\hat{\mathbf{z}}_{\mathbf{n}}$. Thus, $\mathbf{r}$(t) must be along $\hat{\mathbf{y}}'$(t), and precessing with rate $\Omega\,\hat{\mathbf{z}}_{\mathrm{n}}$ in the $\hat{\mathbf{x}}_{\mathbf{n}}\hat{\mathbf{y}}_{\mathbf{n}}$ plane. For $\hat{\mathbf{z}}_{\mathrm{n}}$ to align with $\hat{\mathbf{z}}_{\mathrm{b}}$(t) upon application of rotation vector $\mathbf{r}$(t) and simultaneously comply with the aforementioned constraints, it is required that the magnitude of $\mathbf{r}$(t) be the cone half-angle r. From the rotation sequence in Eq. (4), the initial condition $\mathbf{r}$(0) is parallel to $\hat{\mathbf{y}}_{\mathbf{n}}$. Therefore, the rotation vector $\mathbf{r}$(t) is represented in the reference frame S_n as:

$$\mathbf{r}^{\mathrm{n}} = \begin{bmatrix} -\mathrm{rs}(\Omega t) \\ \mathrm{rc}(\Omega t) \\ 0 \end{bmatrix} \tag{8}$$

and the time argument has been dropped for the sake of simplicity. Recalling Eq. (5), orthogonality of the above $\mathbf{r}$(t) relative to spin axis $\hat{\mathbf{z}}_{\mathrm{b}}$(t) can be verified by:

$$\mathbf{r}^{\mathrm{b}} \cdot \hat{\mathbf{z}}_{\mathbf{b}}^{\mathrm{b}} = (\mathbf{C}_{\mathbf{b}}^{\mathbf{n}}\mathbf{r}^{\mathrm{n}}) \cdot \hat{\mathbf{z}}_{\mathbf{b}}^{\mathrm{b}} = (\mathbf{C}_{\mathbf{b}}^{\mathbf{n}}\mathbf{r}^{\mathrm{n}}) \cdot \begin{bmatrix} 0 \\ 0 \\ 1 \end{bmatrix} = \mathrm{c}(\Omega t)\mathrm{s}(r)(-\mathrm{rs}(\Omega t)) + \mathrm{s}(\Omega t)\mathrm{s}(r)(\mathrm{rc}(\Omega t)) = 0 \tag{9}$$

The spin rate $\dot{\phi}$ in Eq. (7) remains to be determined. From the rotation sequence in Eq. (4) and examination of Figure 1, the following two constraints occur simultaneously:

Constraint C1: At any instant t, $\hat{\mathbf{y}}_{\mathbf{n}}$ *rotates about* $\hat{\mathbf{y}}'(t) = \hat{\mathbf{r}}(t)$ *describing a cone with half-angle* Ωt *until alignment with* $\hat{\mathbf{y}}_{\mathbf{b}}$(t).

Constraint C2: At any instant t, $\hat{\mathbf{x}}_{\mathbf{n}}$ *rotates about* $\hat{\mathbf{y}}'(t) = \hat{\mathbf{r}}(t)$ *describing a cone with half-angle* $\Omega t + \pi/2$ *until alignment with* $\hat{\mathbf{x}}_{\mathbf{b}}$(t).

Analysis of constraints *C1* and *C2* leads to the following relations, respectively:

$$\hat{\mathbf{y}}_{\mathbf{b}} \cdot \hat{\mathbf{r}} = \mathrm{c}(\Omega t) \tag{10a}$$

$$\hat{\mathbf{x}}_{\mathbf{b}} \cdot \hat{\mathbf{r}} = \mathrm{c}(\Omega t + \pi/2) = -\mathrm{s}(\Omega t) \tag{10b}$$

From Eq. (10a) and consideration of Eqs. (5) and (8):

$$\hat{\mathbf{y}}_{\mathbf{b}}^{\mathrm{n}} \cdot \hat{\mathbf{r}}^{\mathrm{n}} = (\mathbf{C}_{\mathbf{n}}^{\mathbf{b}}\hat{\mathbf{y}}_{\mathbf{b}}^{\mathrm{b}}) \cdot \hat{\mathbf{r}}^{\mathrm{n}} = \{(\mathbf{C}_{\mathbf{b}}^{\mathbf{n}})^{\mathrm{T}} \begin{bmatrix} 0 \\ 1 \\ 0 \end{bmatrix}\} \cdot \begin{bmatrix} -\mathrm{s}(\Omega t) \\ \mathrm{c}(\Omega t) \\ 0 \end{bmatrix} = \mathrm{c}(\Omega t) \tag{11}$$

From the last equation results the following constraint on the spin rate vector $\dot{\phi}$:

$$\mathrm{c}(\dot{\phi} t) = \mathrm{c}(\Omega t) \Rightarrow \dot{\boldsymbol{\phi}} = \pm\Omega\hat{\mathbf{z}}_{\mathbf{b}} \tag{12}$$

Proceeding likewise with regard to Eq. (10b) produces:

$$\hat{\mathbf{x}}_{\mathbf{b}}^{\mathrm{n}} \cdot \hat{\mathbf{r}}^{\mathrm{n}} = (\mathbf{C}_{\mathbf{n}}^{\mathbf{b}}\hat{\mathbf{x}}_{\mathbf{b}}^{\mathrm{b}}) \cdot \hat{\mathbf{r}}^{\mathrm{n}} = \{(\mathbf{C}_{\mathbf{b}}^{\mathbf{n}})^{\mathrm{T}} \begin{bmatrix} 1 \\ 0 \\ 0 \end{bmatrix}\} \cdot \begin{bmatrix} -\mathrm{s}(\Omega t) \\ \mathrm{c}(\Omega t) \\ 0 \end{bmatrix} = -\mathrm{s}(\Omega t) \tag{13}$$

and, after comparison with Eq. (12), the following disambiguation results:

$$s(\dot{\phi}t) = -s(\Omega t) \Rightarrow \dot{\boldsymbol{\phi}} = -\Omega\hat{\mathbf{z}}_b \tag{14}$$

The above spin rate vector is a consequence of constraining $\mathbf{r}(t)$ to be orthogonal to the rotating plane $\hat{\mathbf{z}}_b\hat{\mathbf{z}}_n$. Figure 2 shows the solution. Substitution of Eq. (14) in Eq. (7) yields the desired angular rate vector of classic coning motion represented in the body coordinate frame:

$$\boldsymbol{\omega}_b^{bn} = \begin{bmatrix} -\Omega s(r)c(\Omega t) \\ -\Omega s(r)s(\Omega t) \\ \Omega(c(r)-1) \end{bmatrix} \tag{15}$$

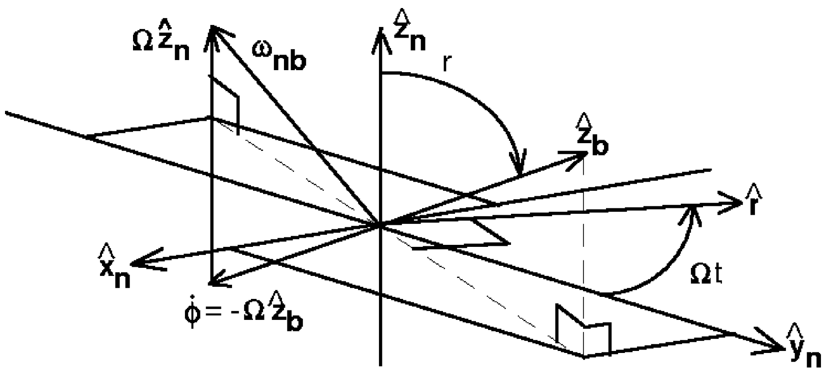

Figure 2- Classic coning motion: spin axis $\hat{\mathbf{z}}_b$ precesses with rate Ω about precession axis $\hat{\mathbf{z}}_n$, maintains constant cone half-angle angle r, and body spin rate $\dot{\phi} = -\Omega$ about spin axis.

The orthogonality between the rotation vector and the above angular rate vector can be inspected by recalling Eqs. (8) and (5), and substitution of Eqs. (14) and (15):

$$\mathbf{r}^b \cdot \boldsymbol{\omega}_b^{bn} = (\mathbf{C}_b^n \mathbf{r}^n) \cdot \boldsymbol{\omega}_b^{bn} = \begin{bmatrix} rs(\dot{\phi}t) \\ rc(\dot{\phi}t) \\ 0 \end{bmatrix} \cdot \boldsymbol{\omega}_b^{bn} = 0 \tag{16}$$

An analogous derivation, this time with the precession rate vector $-\Omega\,\hat{\mathbf{z}}_n$, yields:

$$\boldsymbol{\omega}_b^{bn} = \begin{bmatrix} \Omega s(r)c(\Omega t) \\ -\Omega s(r)s(\Omega t) \\ \Omega(1-c(r)) \end{bmatrix} \tag{17}$$

which is recognized as the angular rate vector usually appearing in the related literature. The motion of angular rate vector $\boldsymbol{\omega}^{bn}$ in space defines a time-varying rotation axis. Figure 3 shows the spatial and body cones generated by $\boldsymbol{\omega}^{bn}$ in Eq. (15). The spatial cone shows the precession of $\boldsymbol{\omega}^{bn}$ about $\hat{\mathbf{z}}_n$ as seen by an observer in S_n. The body cone shows the motion of $\boldsymbol{\omega}^{bn}$ from the point of view of an observer spinning with S_b. The body cone rolls on the surface of the spatial cone, and $\boldsymbol{\omega}^{bn}$ lies along the contact line between both cones. The arrows indicate the spin direction about $\hat{\mathbf{z}}_b$ and the motion of the contact line on the surface of the spatial cone. The cones have no relative motion along the rotation axis; the body cone spins in synch with its rolling motion on the surface of the spatial cone because both movements have frequency Ω.

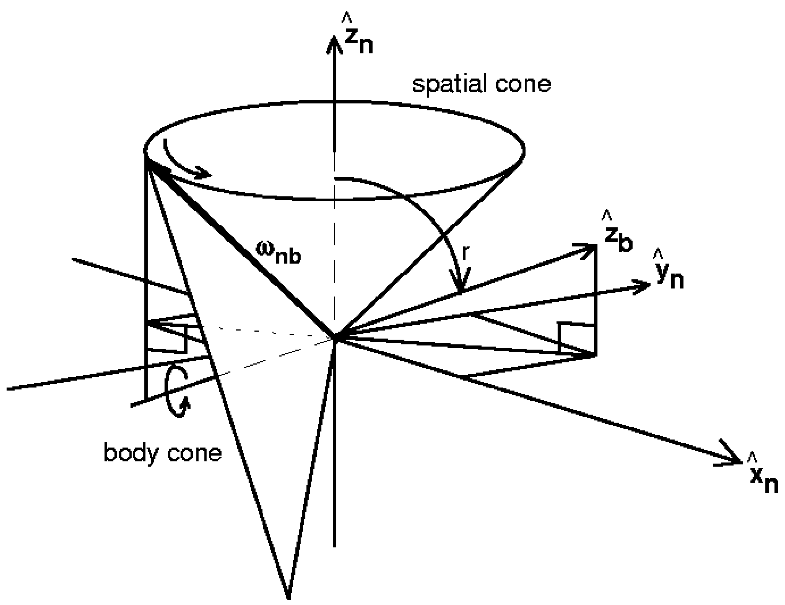

Figure 3 - Body and spatial cones (see Eq.(15)).

3. Conclusion

Classic coning motion is best described as a fairly particular sort of spinning body undergoing precession subject to the rotation vector being orthogonal to the angular rate vector. This work derived the classic coning motion via analysis of a rotation sequence with the appropriate Euler angles. Use of geometry-based reasoning provided an insight into how this particular motion evolves in 3D space. This specific motion is useful to evaluate the accuracy and robustness to finite rotation noncommutativity of candidate attitude determination algorithms for use in inertial navigation systems.

3. Acknowledgement

This work was partially supported by CNPq, Brazil, under the PRONEX grant 015/98 ´Control of Dynamical Systems`, and by Fundação Casimiro Montenegro Filho, grant 94/2002-ITA ´Control Systems for Aerospace Applications`.

4. References

Bortz,J.E., 1971, "A New Mathematical Formulation for Strapdown Inertial Navigation," IEEE Transactions on Aerospace and Electronic Systems, Vol.7, No.1, pp.61-66.

Ignagni, M.B., 1990, "Optimal Strapdown Attitude Integration Algorithms," Journal of Guidance, Control, and Dynamics, Vol.13, No.2, pp.363-369.

Ignagni, M.B., 1994, "On the Orientation Vector Differential Equation in Strapdown Inertial Systems," IEEE Transactions on Aerospace and Electronic Systems, Vol.30, No.4, pp.1076-1081.

Jiang,Y.F. and Lin,Y.P., 1991, "On The Rotation Vector Differential Equation," IEEE Transactions on Aerospace and Electronic Systems, Vol.27, No.1, pp.181-183.

Jiang,Y.F. and Lin,Y.P., 1992, "Improved Strapdown Coning Algorithms," IEEE Transactions on Aerospace and Electronic Systems, Vol.28, No.2, pp.484-490.

Lee,J.G.; Yoon,Y.J.; Mark,J.G. and Tazartes,D.A., 1990, "Extension of Strapdown Attitude Algorithm for High-Frequency Base Motion," Journal of Guidance, Control, and Dynamics, Vol.13, No.4, pp.738-743.

Lovren,N. and Pieper,J.K., 1998, "Error Analysis of Direction Cosines and Quaternion Parameters Techniques for Aircraft Attitude Determination," IEEE Transactions on Aerospace and Electronic Systems, Vol.34, No.3, pp.983-989.

Miller,R.B., 1983, "A New Strapdown Attitude Algorithm," Journal of Guidance, Control, and Dynamics, Vol.6, No.4, pp.287-291.

Pio,R.L., 1966, "Euler Angle Transformations," IEEE Transactions on Automatic Control, Vol.11, No.4, pp.707-715.

Shuster,M.D., 1993, "The Kinematic Equation for the Rotation Vector, " IEEE Transactions on Aerospace and Electronic Systems, Vol.29, No.1, pp.263-267.